ELECTRONIC SUPPLEMENTARY INFORMATION (ESI)

New Atomically Precise M_1Ag_{21} (M = Au/Ag) Nanoclusters as Excellent Oxygen Reduction Reaction Catalysts

Xuejuan Zou,[a,c] Shuping He,[a,c] Xi Kang,[a,c] Shuang Chen,[b,c] Haizhu Yu,[a,c] Shan Jin,[*,b,c] Didier Astruc,[*,d] Manzhou Zhu[*,a,b,c]

a. Department of Chemistry and Centre for Atomic Engineering of Advanced Materials, Anhui Province, Key Laboratory of Chemistry for Inorganic/Organic Hybrid Functionalized Materials, Anhui University, Hefei, Anhui, 230601, P. R. China

b. Institutes of Physical Science and Information Technology, Anhui University, Hefei, Anhui, 230601, P. R. China

c. Key Laboratory of Structure and Functional Regulation of Hybrid Materials（Anhui University), Ministry of Education, Hefei, 230601, P.R. China

d. Université de Bordeaux, 33405 Talence Cedex, France

Table of ESI Contents

I. Synthesis.

Synthesis of $Au_1Ag_{22}(SAdm)_{12}$, $Ag_{25}(2,4\text{-}DMBT)_{18}$, $Au_{25}(PET)_{18}$, $Ag_{29}(PPh_3)_4(BDT)_{12}$, $Ag_{44}(SPhF_2)_{30}$, $Ag_{50}(Dppm)_6(TBBM)_{30}$, Ag-dppf Complexes / Nanoparticles and Ag-SAdm Complexes / Nanoparticles.

The syntheses of the nanoclusters $Au_1Ag_{22}(SAdm)_{12}$,[S1] $Ag_{25}(2,4\text{-}DMBT)_{18}$,[S2] $Au_{25}(PET)_{18}$,[S3] $Ag_{29}(PPh_3)_4(BDT)_{12}$,[S4] $Ag_{44}(SPhF_2)_{30}$,[S5] and $Ag_{50}(Dppm)_6(TBBM)_{30}$[S6] were conducted according to procedures reported in the literature, and these nanoclusters were obtained as described.

The method of synthesis of the nanoparticles Ag-dppf / SAdm was the same as that reported in the literature.[S7] Briefly, 0.2 mmol $AgNO_3$ (33.9 mg) was dissolved in 20 ml CH_3OH, and this solution was cooled to 0°C with slow stirring; then, 0.4 mmol dppf (221mg) or 1-AdmSH (67.2 mg) was added into this solution, and the obtained black precipitate was washed several times with CH_3OH, yielding about 35 mg for Ag-dppf nanoparticles and 18 mg for Ag-SAdm nanoparticles.

The synthesis of Ag-dppf / SAdm complexes was also conducted as in the literature.[S8] Briefly, 0.1 mmol dppf (55 mg) or 1-AdmSH (17 mg) was dissolved with 10 ml CH_3OH, then 0.1 mmol (17.0 mg) $AgNO_3$ in 5 ml CH_3CN was added into the CH_3OH solution, and this reaction mixture was stirred for one day at room temperature. The final solution was evaporated to dryness to provide the complexes (about 15 mg for Ag-dppf complexes and 12 mg for Ag-SAdm complexes).

Preparation of the other activated carbon-supported catalysts. The samples of the other catalysts were fabricated in a similar manner upon employing $Ag_{25}(2,4\text{-}DMBT)_{18}$, $Au_{25}(PET)_{18}$, $Au_1Ag_{22}(SAdm)_{12}$, $Ag_{29}(PPh_3)_4(BDT)_{12}$, $Ag_{44}(SPhF_2)_{30}$, $Ag_{50}(Dppm)_6(TBBM)_{30}$, Ag-dppf complexes / nanoparticles, Ag-SAdm complexes / nanoparticles, and dppf as the respective precursor instead of Ag_{22} or Au_1Ag_{21}. The loading amounts were always 10% on the activated carbon, except that for dppf was 1%. These samples are named as **$Ag_{25}(2,4\text{-}DMBT)_{18}$/C, $Au_{25}(PET)_{18}$/C, $Au_1Ag_{22}(SAdm)_{12}$/C, $Ag_{29}(PPh_3)_4(BDT)_{12}$/C, $Ag_{44}(SPhF_2)_{30}$/C, $Ag_{50}(Dppm)_6(TBBM)_{30}$/C, Ag-dppf Complexes/C, Ag-dppf Nanoparticles/C, Ag-SAdm Complexes/C, Ag-SAdm Nanoparticles/C, and dppf/C.**

II. Physical measurements.

Characterization. The UV/vis. absorption spectra of the nanoclusters dissolved in CH_2Cl_2 were recorded using an Agilent 8453. Electrospray ionization time-of-flight mass spectrometry (ESI-TOF-MS) measurements were performed on a MicroTOF-QIII high-resolution mass spectrometer. X-ray photoelectron spectroscopy (XPS) measurements were performed on Thermo ESCALAB 250. Configuration was with a mono-chromated Al Kα (1486.8 eV) 150 W X-ray source, 0.5 mm circular spot size, a flood gun to counter charging effects, and the analysis chamber base pressure lower than 1×10^{-9} mbar; data were collected with FAT = 20 eV. Thermogravimetric analysis (TGA) was carried out on a thermogravimetric analyzer (DTG-60H, Shimadzu Instruments, Inc.) with 10 mg of nanoclusters in a SiO_2 pan at a heating rate of 10 K min^{-1} from room temperature to 1073 K. Fourier Transform Infrared (FT-IR) spectra were recorded with a Bruker Tensor 27 instrument. Transmission electron microscopy (TEM) was conducted on a JEM-2100 microscope with an accelerating voltage of 200 kV.

Electrochemical measurements (DPV). Electrochemical measurements were performed with an electrochemical workstation (CHI700E) using a Pt working electrode (diameter 0.4 mm), a Pt wire counter electrode, and a Ag wire quasi-reference electrode in 0.1 M Bu_4NPF_6-CH_2Cl_2. Prior to use, the working electrode was polished with 0.05 μm Al_2O_3 slurries and then cleaned by sonication in dilute CH_3CH_2OH and nanopure water successively. The electrolyte solution was deaerated with ultra-high purity nitrogen for 30 min and blanketed under nitrogen atmosphere throughout the experimental procedure.

III. Supporting Figures.

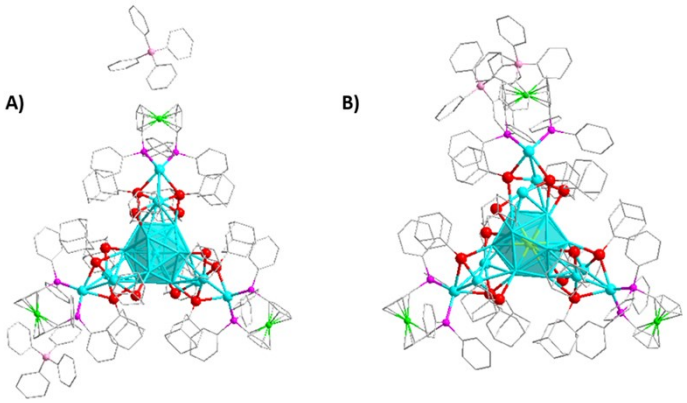

Figure S1. The whole structures of A) $Ag_{22}(dppf)_3(SAdm)_{12}(BPh_4)_2$ and B) $Au_1Ag_{21}(dppf)_3(SAdm)_{12}(BPh_4)_2$. The H atoms are omitted for clearly. Color labels: yellow = Au; blue = Ag; red = S; purple = P; green = Fe; pink = B; gray = C.

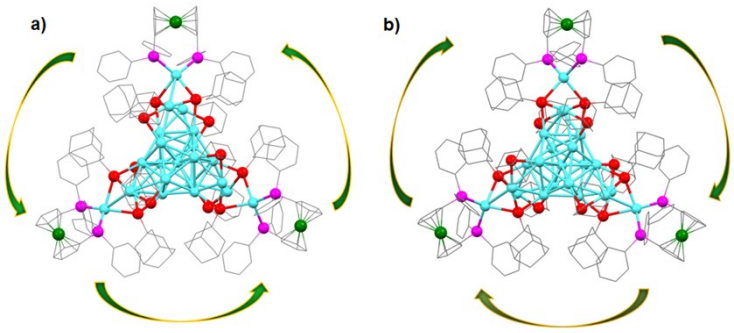

Figure S2. Enantiomers of $[Ag_{22}(dppf)_3(SAdm)_{12}]^{2+}$ in the unit cell.

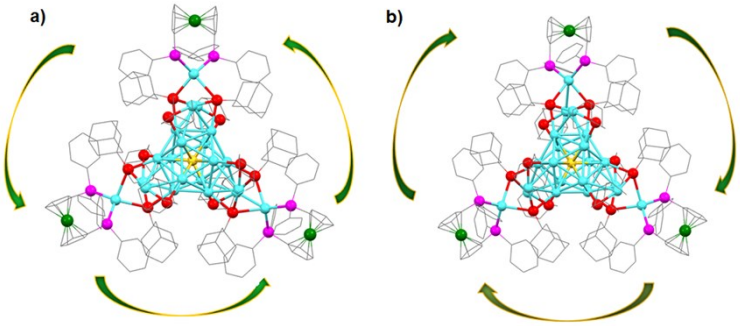

Figure S3. Enantiomers of $[Au_1Ag_{21}(dppf)_3(SAdm)_{12}]^{2+}$ in the unit cell.

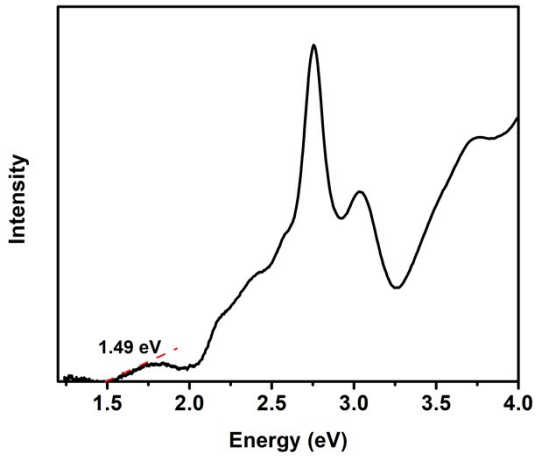

Figure S4. Optical absorption spectrum of $Ag_{22}(dppf)_3(SAdm)_{12}$.

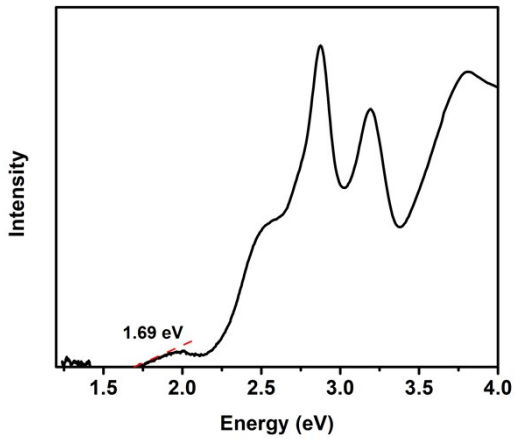

Figure S5. Optical absorption spectrum of $Au_1Ag_{21}(dppf)_3(SAdm)_{12}$.

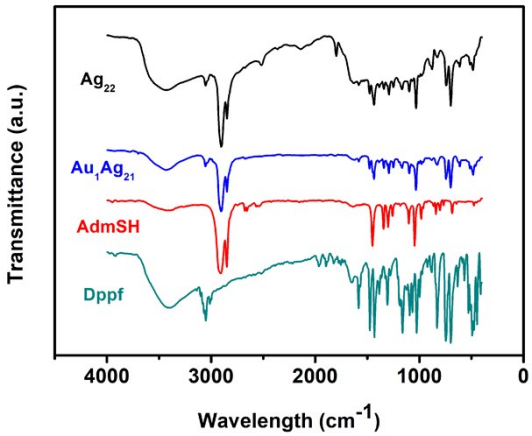

Figure S6. FT-IR spectra of $[Ag_{22}(dppf)_3(SAdm)_{12}](BPh_4)_2$, $[Au_1Ag_{21}(dppf)_3(SAdm)_{12}](BPh_4)_2$, 1, 1'-bis(diphenylphosphino)ferrocene, and 1-adamantanethiol.

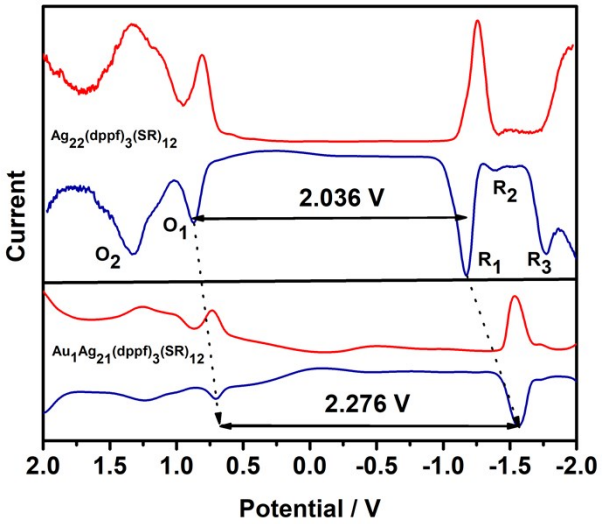

Figure S7. Differential pulse voltammetry spectra of $[Ag_{22}(dppf)_3(SAdm)_{12}](BPh_4)_2$ and $[Au_1Ag_{21}(dppf)_3(SAdm)_{12}](BPh_4)_2$ nanoclusters.

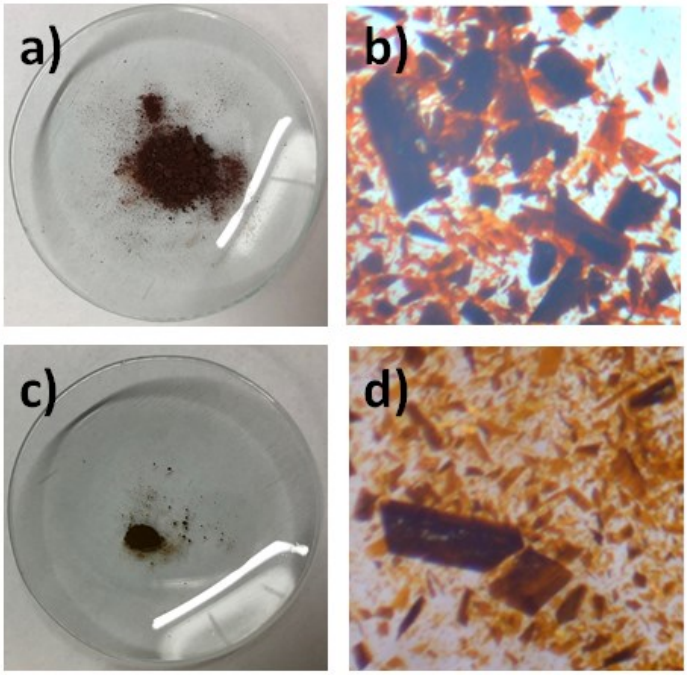

Figure S8. Digital pictures of powders and crystals for a), b) Ag_{22} and c), d) for Au_1Ag_{21}.

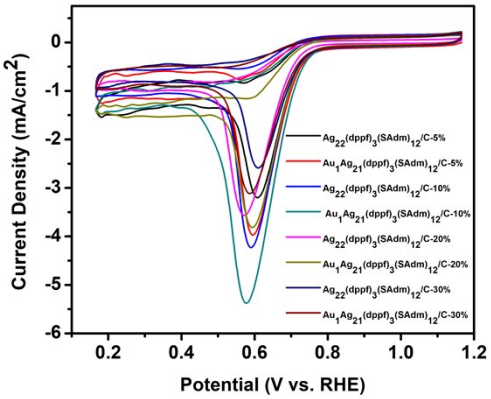

Figure S9. CV curves of Ag_{22} and Au_1Ag_{21} NCs with different loading in 0.1 M KOH saturated with O_2.

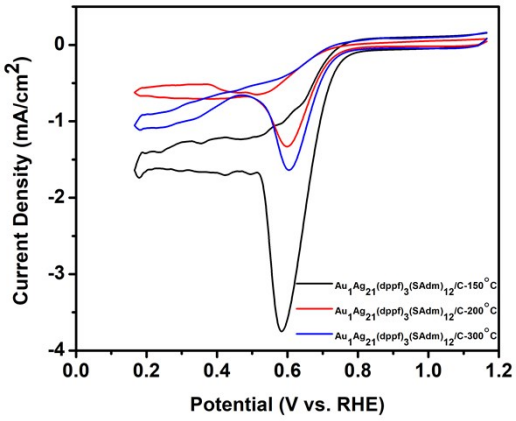

Figure S10. CV curves of $Au_1Ag_{21}(dppf)_3(SAdm)_{12}$/C after calcination at 150, 200 and 300 °C in 0.1 M KOH saturated with O_2. The loading was 10% and the scan rate was 0.05 V s^{-1}.

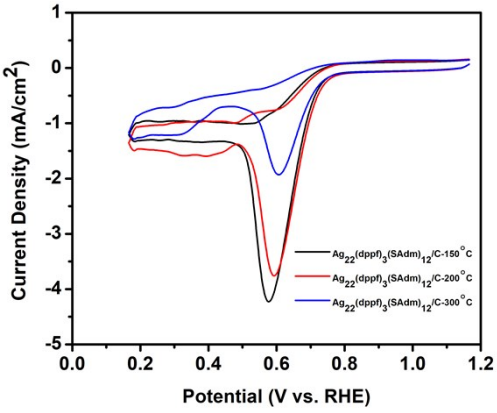

Figure S11. CV curves of $Ag_{22}(dppf)_3(SAdm)_{12}$/C after treating with 150, 200 and 300 °C in 0.1 M KOH saturated with O_2.

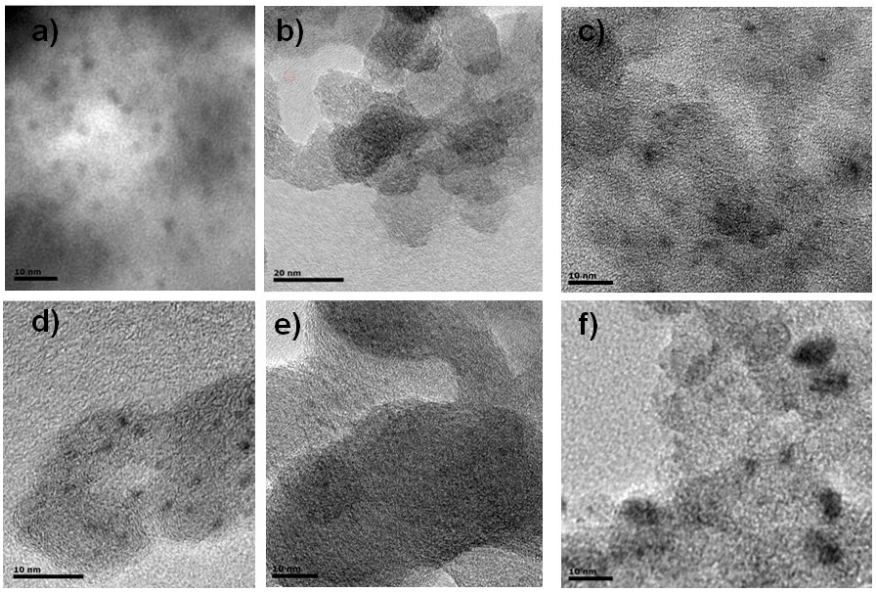

Figure S12. TEM images of $Ag_{22}(dppf)_3(SAdm)_{12}$/C and $Au_1Ag_{21}(dppf)_3(SAdm)_{12}$/C before (a, d) and after calcination at 150 (b, e) and 300 °C (c, f).

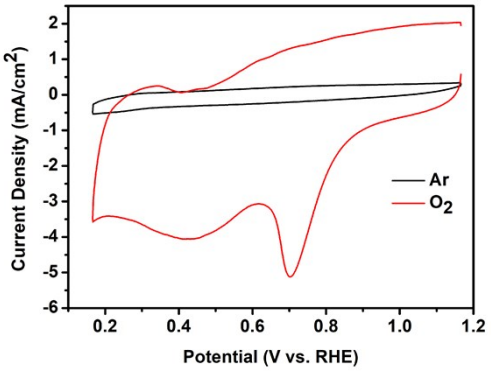

Figure S13. CV curves of the commercial Pt/C in 0.1 M KOH saturated with Ar and O_2.

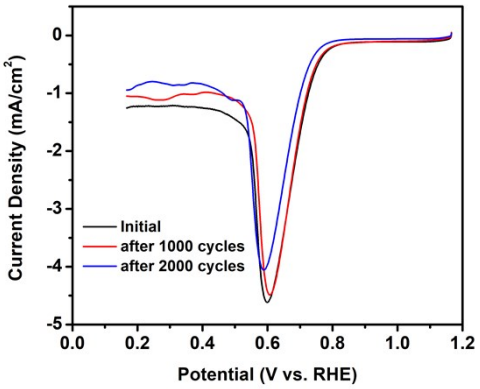

Figure S14. ORR polarization curves of $Ag_{22}(dppf)_3(SAdm)_{12}$/C after 1000 and 2000 cycles.

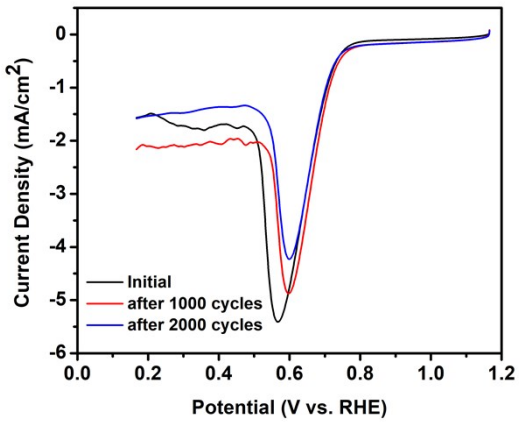

Figure S15. ORR polarization curves of $Au_1Ag_{21}(dppf)_3(SAdm)_{12}$/C after 1000 and 2000 cycles.

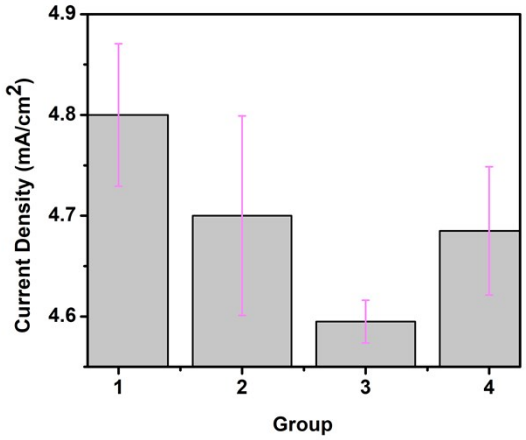

Figure S16. Reproducibility and level of error analysis for $Ag_{22}(dppf)_3(SAdm)_{12}$/C.

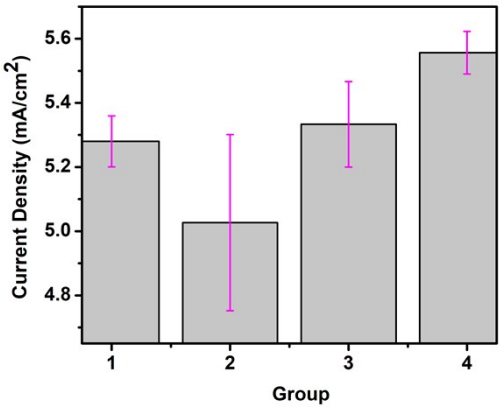

Figure S17. Reproducibility and level of error analysis for $Au_1Ag_{21}(dppf)_3(SAdm)_{12}$/C.

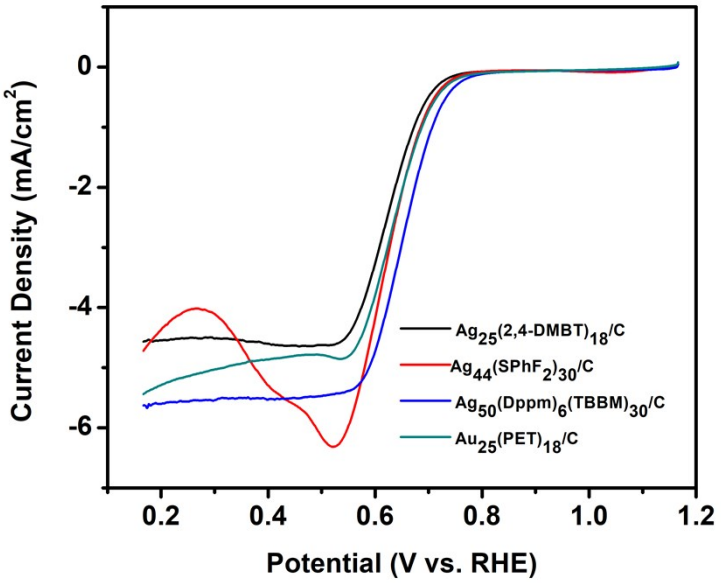

Figure S18. RDE voltammograms of $Ag_{25}(2,4\text{-DMBT})_{18}$/C, $Ag_{44}(SPhF_2)_{30}$/C, $Ag_{50}(Dppm)_6(TBBM)_{30}$/C, and $Au_{25}(PET)_{18}$/C in 0.1 M KOH solution saturated with oxygen at the rotation rate of 2500 rpm.

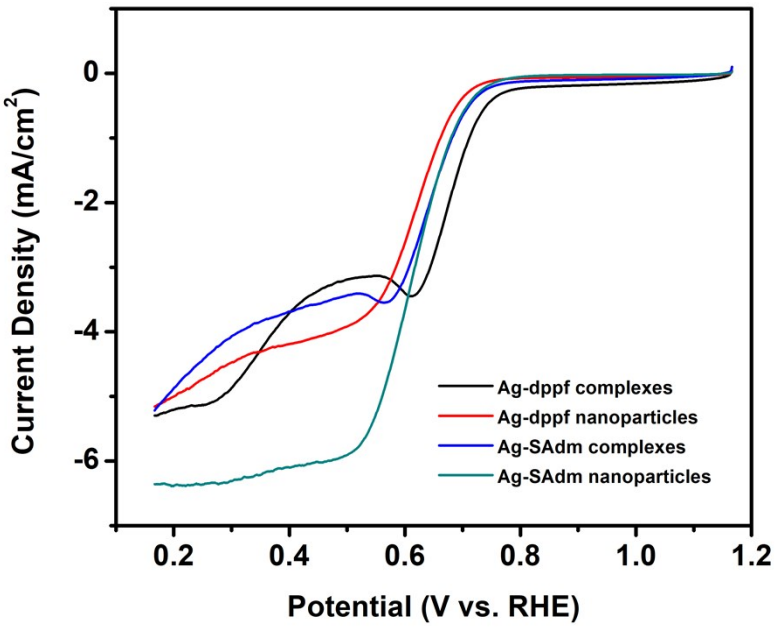

Figure S19. RDE voltammograms of Ag-dppf complexes/C, Ag-dppf nanoparticles/C, and Ag-SAdm complexes /C, Ag-SAdm nanoparticles/C in 0.1 M KOH solution saturated with oxygen at the rotation rate of 2500 rpm.

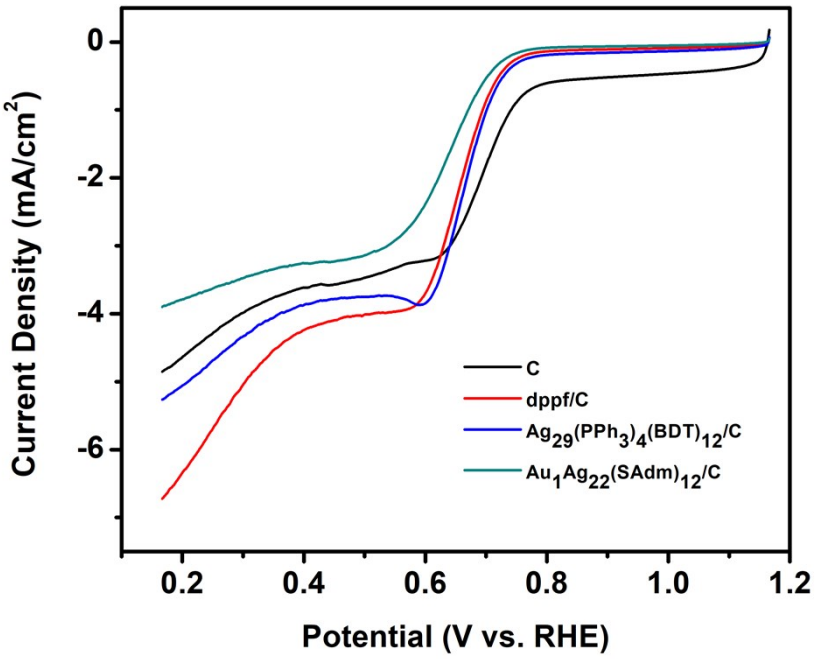

Figure S20. RDE voltammograms of activated carbon (C), dppf/C, $Ag_{29}(PPh_3)_4(BDT)_{12}$/C, and $Au_1Ag_{22}(SAdm)_{12}$/C in 0.1 M KOH solution saturated with oxygen at the rotation rate of 2500 rpm.

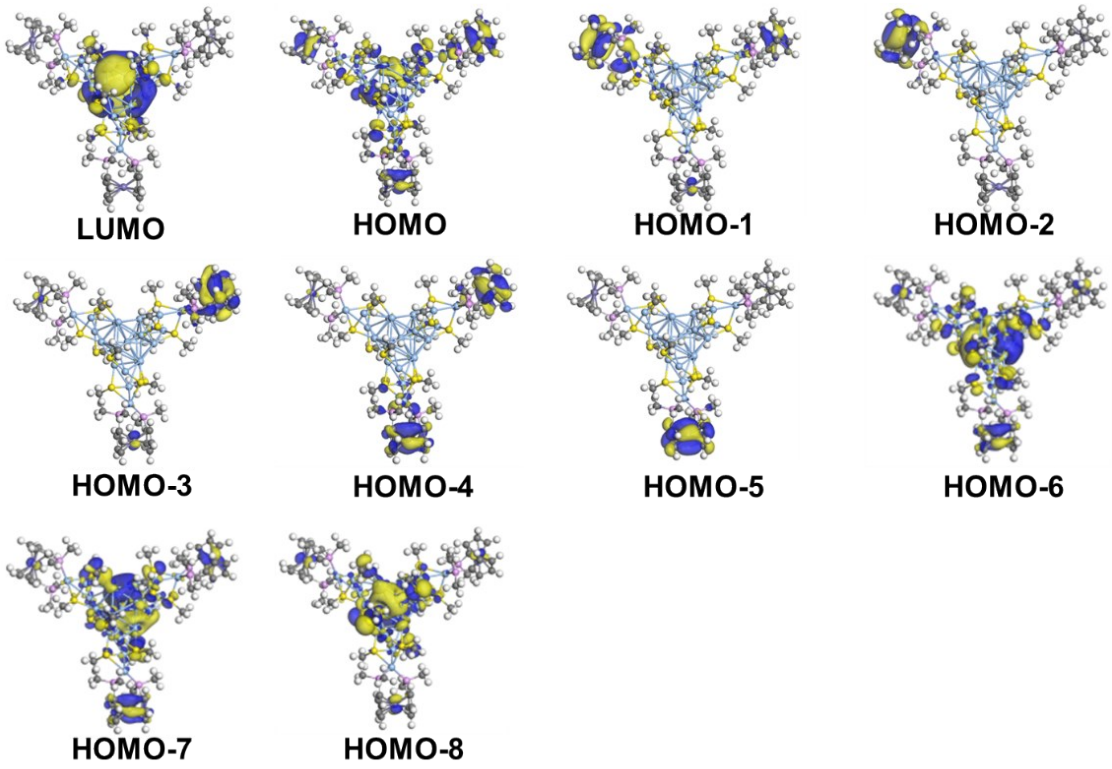

Figure S21. Full details of the HOMOs of $Ag_{22}(dmpf)_3(SMe)_{12}$.

Table S1. Peak potentials (E_p) and peak current density (j_P) of Ag_{22} and Au_1Ag_{21} NCs with different loading.

Sample	5%	10%	20%	30%
$Ag_{22}(dppf)_3(SAdm)_{12}/C$	3.19 (mA/cm^2) 0.61 V	4.23 (mA/cm^2) 0.59 V	3.57 (mA/cm^2) 0.57 V	2.58 (mA/cm^2) 0.61 V
$Au_1Ag_{21}(dppf)_3(SAdm)_{12}/C$	3.95 (mA/cm^2) 0.59 V	5.38 (mA/cm^2) 0.57 V	3.81 (mA/cm^2) 0.59 V	3.12 (mA/cm^2) 0.58 V

Table S2. Peak potentials (E_p) and peak current density (j_P) of $Ag_{22}(dppf)_3(SAdm)_{12}/C$ and $Au_1Ag_{21}(dppf)_3(SAdm)_{12}/C$ after calcination at different temperatures.

Sample	150℃	200℃	300℃
$Ag_{22}(dppf)_3(SAdm)_{12}/C$	4.23 (mA/cm^2) 0.57 V	3.76 (mA/cm^2) 0.59 V	1.92 (mA/cm^2) 0.60 V
$Au_1Ag_{21}(dppf)_3(SAdm)_{12}/C$	3.75 (mA/cm^2) 0.58 V	1.33 (mA/cm^2) 0.60 V	1.63 (mA/cm^2) 0.60 V

Table S3. Comparison of the ORR activities of $M_1Ag_{21}(dppf)_3(SAdm)_{12}/C$ with materials in other reported works in alkaline solutions.

Sample	E_p (V)	j_p (mA cm^{-2})	E_{onset} (V)	Scan rate	ref
$Ag_{22}(dppf)_3(SAdm)_{12}/C$	0.59	4.23	0.82	0.05	this work
$Au_1Ag_{21}(dppf)_3(SAdm)_{12}/C$	0.57	5.38	0.86	0.05	this work
g-C_3N_4	0.166	1.40	0.76	--	(S9)
g-C_3N_4@CMK-3	0.716	6.0	0.866	--	(S9)
N-S-G	0.716	3.0	0.866	--	(S10)
B,N-graphene	0.686	4.2	0.86	0.1	(S11)
h-BN/graphene	0.586	2.5	0.746	0.1	(S11)
P-ACNT	0.658	1.8	0.808	0.1	(S12)
N-ACNT	0.708	2.6	0.858	0.1	(S12)
PN-ACNT	0.86	2.9	0.878	0.1	(S12)
CoO/NCNT	0.86	--	0.93	0.02	(S13)
$MnCo_2O_4$/N-rmGO	0.88	0.8	0.95	0.05	(S14)
Co_3O_4/N-mGO	0.86	0.6	0.93	0.05	(S14)

Table S4. Crystal Data and Structure Refinement for $[Ag_{22}(dppf)_3(SAdm)_{12}](BPh_4)_2$.

Chemical formula	$C_{222}H_{264}Ag_{22}Fe_3P_6S_{12}$•$2(C_{24}H_{20}B)$•$3(C_7H_8)$•$C_7H_5$
Formula Mass	7047.47
Crystal system	triclinic
a/Å	21.4120(2)
b/Å	27.2727(3)
c/Å	29.7612(3)
α/°	79.1230(10)
β/°	70.4930(10)
γ/°	66.9560(10)
Unit cell volume/Å^3	15041.0(3)
Temperature/K	150
Space group	P -1
No. of formula units per unit cell, Z	2
No. of reflections measured	155377
No. of independent reflections	52178
R_{int}	0.0452
Final R_1 values ($I > 2\sigma(I)$)	0.0741
Final $wR(F^2)$ values ($I > 2\sigma(I)$)	0.1974
Final R_1 values (all data)	0.0872
Final $wR(F^2)$ values (all data)	0.2054

Table S5. Crystal Data and Structure Refinement for $[Au_1Ag_{21}(dppf)_3(SAdm)_{12}]$ $(BPh_4)_2$.

Chemical formula	$C_{285}H_{325}Ag_{21}AuB_2Cl_2Fe_3O_2P_6S_{12}$
Formula Mass	7074.29
Crystal system	triclinic
a/Å	21.3948(19)
b/Å	27.211(3)
c/Å	29.938(4)
α/°	80.347(10)
β/°	70.094(9)
γ/°	67.283(8)
Unit cell volume/Å^3	15103(3)
Temperature/K	120(2)
Space group	P -1
No. of formula units per unit cell, Z	2
No. of reflections measured	80621
No. of independent reflections	42924
R_{int}	0.0793
Final R_1 values ($I > 2\sigma(I)$)	0.1160
Final $wR(F^2)$ values ($I > 2\sigma(I)$)	0.3142
Final R_1 values (all data)	0.1413
Final $wR(F^2)$ values (all data)	0.3333

IV. References

(1) S. Chen, W. Du, C. Qin, D. Liu, L. Tang, Y. Liu, S. Wang and M. Zhu, *Angew. Chem. Int. Ed.,* 2020, **59**, 7542 – 7547.

(2) M. S. Bootharaju, C. P. Joshi, M. R. Parida, O. F. Mohammed and O. M. Bakr, *Angew. Chem. Int. Ed.,* 2016, **55**, 922.

(3) C. Yao, J. Chen, M. -B. Li, L. Liu, J. Yang and Z. Wu, *Nano Lett.,* 2015, **15**, 1281-1287.

(4) L. G. AbdulHalim, M. S. Bootharaju, Q. Tang, S. DelGobbo, R. G. AbdulHalim, M. Eddaoudi, D.-e. Jiang and O. M. Bakr, *J. Am. Chem. Soc.,* 2015, **137**, 11970.

(5) H. Yang, Y. Wang, H. Huang, L. Gell, L. Lehtovaara, S. Malola, H. Häkkinen and N. Zheng, *Nat. Commun.,* 2013, **4**, 2422.

(6) W. Du, S. Jin, L. Xiong, M. Chen, J. Zhang, X. Zou, Y. Pei, S. Wang and M. Zhu, *J. Am. Chem. Soc.,* 2017, **139**, 1618-1624.

(7) Y. Lee, A. Loew and S. Sun, *Chem. Mater.,* 2010, **22**, 755-761.

(8) Y. Qu, K. Zhao, C. Wang, Y. Wu, L. Xia and H. Wu, *J. Mol. Struct.,* 2020, **1203**, 127424.

(9) Y. Zheng, Y. Jiao, J. Chen, J. Liu, J. Liang, A. Du, W. Zhang, Z. Zhu, S. C. Smith, M. Jaroniec, G. Lu and S. Qiao, *J. Am. Chem. Soc.,* 2011, **133**, 20116-20119.

(10) J. Liang, Y. Jiao, M. Jaroniec and S. Qiao, *Angew. Chem. Int. Ed.,* 2012, **51**, 11496 -11500.

(11) Y. Zheng, Y. Jiao, L. Ge, M. Jaroniec and S. Qiao, *Angew. Chem. Int. Ed.,* 2013, **52**, 3110-3116.

(12) D. Yu, Y. Xue and L. Dai, *J. Phys. Chem. Lett.,* 2012, **3**, 2863-2870.

(13) Y. Liang, H. Wang, P. Diao, W. Chang, G. Hong, Y. Li, M. Gong, L. Xie, J. Zhou, J. Wang, T. Z. Regier, F. Wei and H. Dai, *J. Am. Chem. Soc.,* 2012, **134**, 15849-15857.

(14) Y. Liang, H. Wang, J. Zhou, Y. Li, J. Wang, T. Regier and H. Dai, *J. Am. Chem. Soc*., 2012, **134**, 3517-3523.